International Journal of Modern Manufacturing Technologies
ISSN 2067–3604, Vol. XVIII, No. 1 / 2026
https://doi.org/ 10.54684/ijmmt.2026.18.1.25

# THE EFFECTS OF TECHNOLOGICAL PARAMETERS ON DIE-FILLING CAPABILITY AND WALL THICKNESS VARIATION IN HYDROFORMING OF NECKED-SPHERICAL COPPER PARTS

**Nguyen Xuan Diep[1], Nguyen Manh Tien[1], Nguyen Truong An[1], Nguyen Xuan Hung[2], Chu Van Huy[1]**

[1]Faculty of Mechanical Engineering, Le Quy Don Technical University, 236 Hoang Quoc Viet Street, Hanoi 100000, Vietnam
[2]Center of Advanced Technology, Le Quy Don Technical University, 236 Hoang Quoc Viet Street, Hanoi 100000, Vietnam

Corresponding author: Nguyen Manh Tien, manhtiennguyen84@lqdtu.edu.vn

***Abstract:*** Current hydroforming research predominantly focuses on symmetric T-shaped or bulged tubular components. The formation of a spherical part from a closed-end cup blank—where sealing and axial compensation are restricted to a single side—remains under-investigated. This study evaluates the impact of internal forming pressure (p) and axial punch velocity (v) on die-filling capability and wall thickness variation in a necked-spherical copper part. A second-order orthogonal experimental design was employed to analyze parameter interactions within this single-sided feeding mechanism. FEM simulations using DEFORM software reveal that while a minimum pressure of 30 MPa is required for die filling without axial feeding, localized deformation leads to premature bursting. Integrating a punch velocity of v = 1–5 mm/s necessitates a pressure range of 45–55 MPa for complete filling. Analytical results confirm that punch velocity exerts a more substantial influence on the wall thinning ratio than forming pressure. Optimization identifies the ideal parameters at p = 45 MPa and v = 5 mm/s, successfully limiting the maximum thinning ratio to 22.1%. These findings provide a critical technical framework for industrial cup-blank hydroforming applications.
***Key words:*** hydroforming, forming pressure, necked-spherical part, die-filling capability, wall thickness variation.

## 1. INTRODUCTION

Copper alloys are currently widely utilized in metal forming research due to their good ductility, allowing for large plastic deformation in a single operation without failure, [1-5]. This facilitates quantitative studies more effectively. Furthermore, copper can be processed in both cold and hot states, and appropriate processing regimes can produce fine-grained structures. Blanks used in research vary from sheets, bars, and tubes. For tubular blanks, the studies are mainly conducted using the hydroforming method.

Tube hydroforming is an advanced manufacturing technology that enables the production of hollow, thin-walled components with complex geometries, high precision, and good mechanical properties, which can be applied to reduce the structural weight of parts, [6-12]. Thanks to its outstanding advantages in product mechanical properties as well as its technological capabilities, hydroforming is applied in various fields, particularly in the automotive, motorcycle, and aerospace industries. For this reason, research on this technology has been widely conducted globally.

Numerous studies on the forming of complex-shaped parts from tubular blanks, [13-21], have been carried out. These include investigations into the stress-strain states at various locations on the blank during hydroforming to determine deformation parameters and die geometries, aiming to minimize defects when forming T-shaped parts. Additionally, many studies have been conducted to investigate the influence of process parameters such as the friction coefficient, initial blank thickness, forming pressure, and axial feeding amount on the formability of T-branches. These studies have also been performed on various materials such as SUS304, aluminum alloys, and copper alloys.

In recent years, research has focused on optimizing pressure paths in hydrostatic stamping. Authors Yong Xu et al. conducted research on optimizing loading paths when stamping pipe blanks from 5A02 aluminum alloy with different blank diameters, [22]. Based on the optimized loading path, the thinning process of the pipe was significantly reduced, increasing the forming ability when stamping 5A02 aluminum alloy pipe blanks. Trinh et al. [23, 24] established mathematical models to predict the forming pressure for T-shaped and cross-shaped parts, emphasizing the role of axial pressing force in compensating for material in the deformation zone.

In addition, modern optimization methods such as Machine Learning [25] and genetic algorithms [26] have also been applied to find the optimal combination between forming pressure and the displacement of the stamping die. For copper material, Vu and colleagues [27] showed that the "working range" of forming pressure directly affects the mold filling ability and the thinning of the pipe wall.

Chunmei Liu and colleagues also conducted research on critical forming ability and predicted failure during hydrostatic stamping of pipe billets, [28]. The failure models were compared, evaluated by simulation and experimentally verified to select a suitable model for the hydrostatic stamping of pipe billets in the future.

Current studies are primarily conducted using numerical simulation methods or a combination of numerical simulation and experiments. Taking advantage of numerical simulation, it is possible to determine suitable sets of process parameters to form parts as required, predict potential defects, and consequently provide recommendations to ensure product quality. Experimental procedures are mainly carried out to verify simulation results and to establish appropriate technological processes for specific materials and production conditions.

Research on forming hollow parts from tubular blanks via hydroforming has also been conducted at various temperature states, including cold forming, warm forming, and multi-stage forming combined with intermediate annealing to eliminate strain hardening. However, current studies predominantly focus on forming bulged products or T-shaped products from hollow tubular blanks. There is limited research on forming spherical parts from cup-shaped blanks, a type of component where the punch pressing process—intended to seal and feed material into the thinning zone—is executed from only one side. Moreover, the effects of parameters such as forming pressure, axial punch speed, etc., are mostly studied and evaluated individually for each input factor or established using simple linear models, which do not fully evaluate the impact of each factor or their interaction effects.

This paper focuses on investigating the influence of several process parameters, including forming pressure (p) and axial punch speed (v), on the die-filling capability and wall thickness variation (degree of wall thinning) when hydroforming a necked-spherical part from a copper cup blank. Based on the obtained results, regression equations are established. Utilizing a second-order orthogonal experimental design, the process parameters are evaluated, selected, and optimized to obtain a completely formed product with the minimum wall thickness variation.

## 2. MATERIALS AND METHODS

### 2.1. Workpiece material

The material used in the simulation is CDA110 copper. The dependence of flow stress (deformation resistance) on the strain rate at 1, 10, and 50 s−1 at a temperature of 20°C is illustrated in Figure 1.

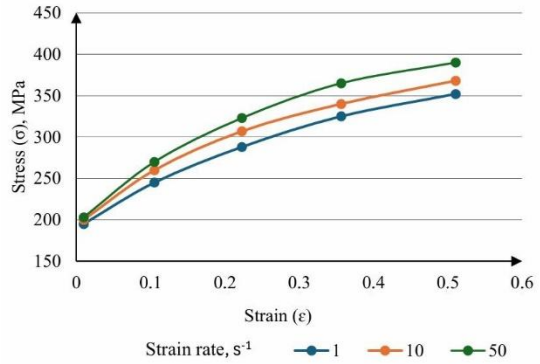


Fig. 1. Stress-strain curves for strain-rate-dependency tests at 20oC of CDA110 copper, [29]

### 2.1. Simulation model

The initial blank is cup-shaped with an outer diameter of 22.2 mm, a wall thickness of 1.2 mm, and a length of 65 mm. The target product is a hollow necked-spherical part with a spherical radius *Rc*=20 mm. Since this is an axisymmetric part, the geometric models of the initial tube blank and die tools were constructed using 2D CAD software and subsequently imported into the Deform software environment for simulation (Figure 2(a) and Figure 2(b)). The hydroforming system consists of a rigid die set, an axial punch, and a cup-shaped copper blank subjected to internal hydraulic pressure. During the forming process, the internal pressure was uniformly applied to the inner surface of the blank, while the axial punch simultaneously supplied material from one side to compensate for wall thinning in the deformation zone. The die and punch were modeled as rigid bodies, whereas the blank was modeled as a deformable plastic material. The hydroforming system model is illustrated in Figure 2(a) and Figure 2(b).

The behavior model of the copper material CDA110 is built according to the plastic-hardening model using equation (1). In which, σ is stress, ε is the degree of strain, K is the strain hardening level (MPa), and n is the strain hardening coefficient. Based on the stress-strain curve (Figure 1), the values of the coefficients are determined accordingly: K=199 MPa, n=0.348.

$$\sigma_i = K\varepsilon_i^n \tag{1}$$

The blank was initially meshed with 2,000 tetrahedral elements, with automatic remeshing triggered to adapt to different deformation zones during the simulation.

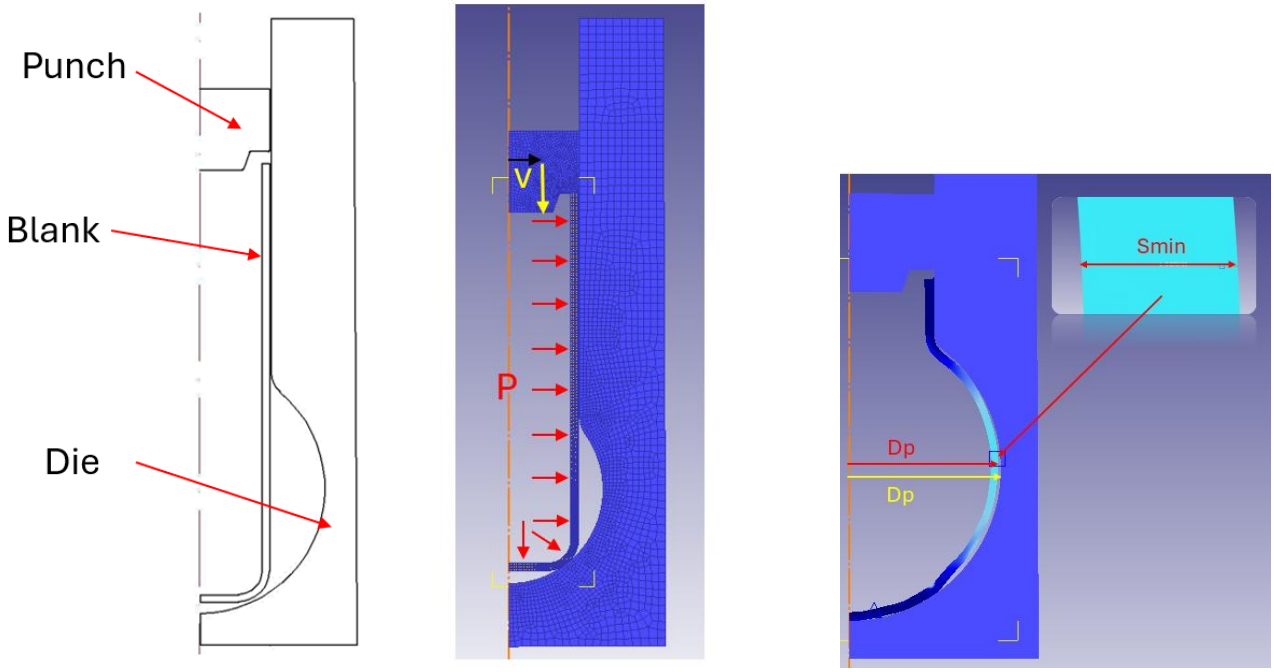


Fig. 2. Geometric model (a), meshed model for simulation (b), and wall thickness measurement (c)

**2.3. Research methodology**

The study was conducted using DEFORM software Version 11.0, specialized for simulating metal forming processes.

Forming pressure is a critical parameter affecting the material's ability to fill the die. When the blank is not subjected to axial compressive force (the punch only functions to maintain internal pressure), the forming pressure can be calculated using equation (2), [30]:

$$P_{TH} = \frac{S_0}{R_{SP}}\sigma_s' \tag{2}$$

Additionally, the bursting pressure of the material can also be determined using equation (3) to select an appropriate value range, avoiding fracture defects during the forming process:

$$P_b = \frac{S_0}{R_{SP}}\sigma_b \tag{3}$$

where: $P_{TH}$ – forming pressure (MPa); - $S_0$ – initial wall thickness (mm); $R_{SP}$ – minimum fillet radius of the product (mm); $\sigma_s'$ – flow stress of the material (MPa); $P_b$ – fracture pressure (MPa); $\sigma_b$ - tensile strength of the material (MPa).

The effects of process parameters, including forming pressure (p) and axial punch speed (v) were investigated independently through simulations to find suitable variation ranges. The initial range of forming pressure values was selected based on calculations using formulas (2-3); however, since the blank is axially compressed during deformation, the actual value is typically higher. To find the appropriate values when changing the punch speed

from 1 - 5 mm/s, the forming pressure was set to gradually increase from an initial pressure of 25 MPa in increments of 5 MPa. In DEFORM software, the forming pressure is applied across the entire inner surface of the workpiece (Figure 2(b)), where a negative value is input to comply with the software's sign convention, ensuring the pressure vector is directed outwards.
The technological parameters and boundary conditions for the hydroforming simulation are selected as shown in Table 1.

Table 1. Technological parameters used in the simulation

| Technological parameters | Value |
|---|---|
| Number of finite elements | 2000 |
| Tool materials | SKD11 |
| Coefficient of friction | 0.1 |
| Ambient temperature, °C | 20 |

The die filling capability is evaluated based on the percentage ratio of the obtained product diameter to the die diameter $D_p/D_d$; while the degree of wall thickness variation after forming is evaluated based on the percentage ratio of the change in wall thickness at the thinnest location to the initial wall thickness $(S_o - S_{min})/S_o$, (Figure 2(c)).

## 3. RESULTS AND DISCUSSION

### 3.1. Effect of forming pressure on die-filling capability and wall thickness variation

The investigation into the effect of forming pressure on the die-filling capability without an axial feeding forcewas conducted with various pressure values. The research results are presented in the chart in Figure 3.

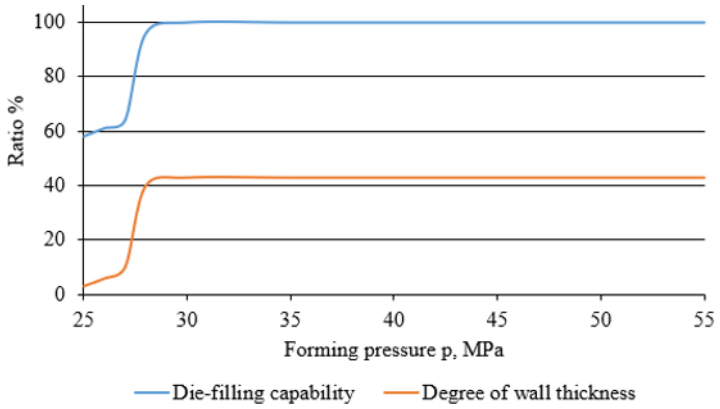


Fig. 3. Effect of forming pressure on formability and wall thickness variation

The results indicate that, in the absence of an axial feeding force, when the forming pressure is 25 MPa (according to formula (2)), the die filling ratio reaches 58%. This means that a pressure of 25 MPa is only sufficient to initiate deformation of the blank, not enough to fill the die cavity. When the forming pressure increases to a certain value (p = 30 MPa), the blank fills the die cavity. At this point, the degree of wall thinning increases from 3 to 43%. Continuing to increase the pressure p, it can be observed that the degree of wall thinning remains unchanged. This proves that the deformation process without an axial feeding force only occurs locally around the maximum bulging area of the blank.
However, a 43% variation in wall thickness may cause fracture (bursting) when hydroforming copper tubular blanks. Therefore, to ensure that the blank does not burst during forming, it is necessary to feed material from the tube end to compensate for the thinning zone by applying an axial feeding force.
Due to the increased wall thickness and work hardening during axial feeding, the forming pressure required for die-filling also increases. At a punch speed of 5 mm/s, simulation results indicate that a minimum pressure of 45 MPa is required to fill the die cavity. Consequently, subsequent simulation studies were conducted within a forming pressure range of 45–55 MPa to ensure successful cavity filling.

### 3.2. Effect of axial punch velocity on wall thickness variation

To ensure that wrinkling defects do not occur on the blank during deformation, the axial punch velocity is selected within the range of 1 to 5 mm/s. Through the simulation method, the minimum forming pressure required to

ensure complete die cavity filling when the punch moves at a speed in the range of 1÷5 mm/s is determined to be p = 45 MPa.
The study on the effect of axial punch velocity on the wall thickness variation when the forming pressure p = 45 MPa was conducted via simulation with a speed increment of 1 mm/s. The simulation results are shown in the image map in Figure 4 and the chart in Figure 5.
According to the Cockroft-Latham failure criterion, an increase in axial feeding speed from 1 to 5 mm/s leads to a reduction in the damage factor from 0.74 to 0.63. In the case of CDA110 copper hydroforming, these calculated factors are well within the permissible deformation limits.

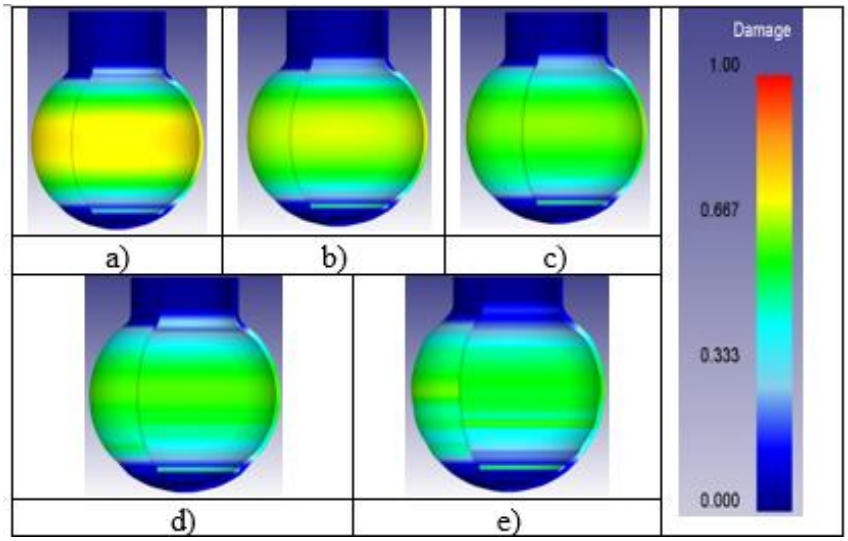


Fig. 4. Material damage factor under 45 MPa pressure at different axial punch velocities: v=1mm/s (a), v=2mm/s (b), v=3mm/s (c), v=4mm/s (d), v=5mm/s (e)

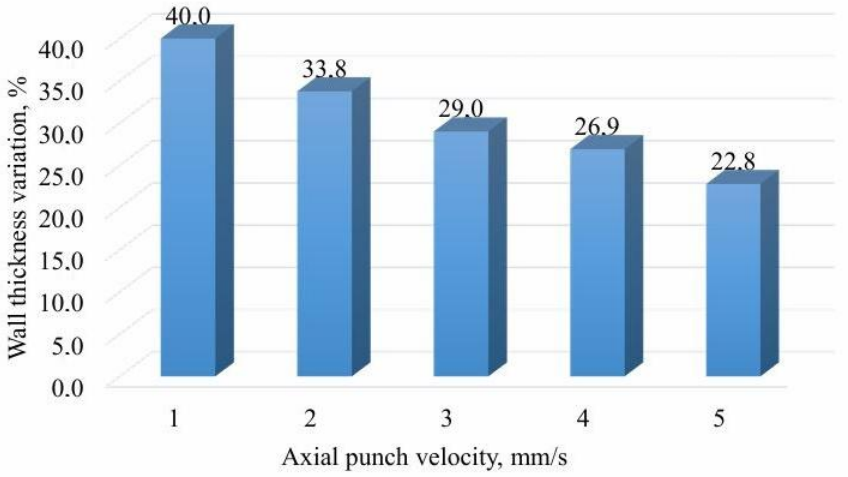


Fig. 5. Effect of axial punch velocity under 45 MPa pressure on the wall thickness variation

According to the damage distribution maps in Figure 4, it is evident that increasing the axial punch velocity leads to a reduction in the material damage factor. This trend aligns with the wall thickness variation results presented in Figure 5. Specifically, as the punch velocity increases from 1 mm/s to 5 mm/s, the maximum wall thinning decreases significantly from 40% to 22.8% (Figure 4).
Within this range of punch velocities, simulations were conducted to determine the appropriate forming range (where no wrinkling or fracturing defects occur during the forming process). Based on simulation results obtained by comparing the material failure coefficients, the maximum forming pressure value determined is 55 MPa.

### 3.3. Simulation Planning and Optimization

#### 3.3.1. Formulation of the simulation-based optimization problem

To achieve the smallest change in wall thickness, the technological parameters were planned and optimized based on simulation results.

To fully assess the influence of individual technological parameters (forming pressure (p) and axial punch velocity (v)), as well as the interaction between them, the second-order orthogonal planning method was chosen. Based on the simulation, the range of influence values of the selected factors was coded and shown in Table 3.

Table. 3. Factors affecting the degree of wall thickness change

| *Factors* | *Forming pressure (p), [MPa]* | *Punch velocity (v), [mm/s]* |
|---|---|---|
| | $X_1$ | $X_2$ |
| $x_i$= -1 | 45 | 1 |
| $x_i$= +1 | 55 | 5 |

The simulation was conducted according to the simulation matrix presented in Table 4, with the objective function $Y$ defined as the minimization of wall thickness variation.

Table 4. Planning matrix

| *№* | *$X_1$* | *$X_2$* | *Y* |
|---|---|---|---|
| 1 | -1 | -1 | |
| 2 | +1 | -1 | |
| 3 | -1 | +1 | |
| 4 | +1 | +1 | |
| 5 | -1.414 | 0 | |
| 6 | +1.414 | 0 | |
| 7 | 0 | -1.414 | |
| 8 | 0 | +1.414 | |
| 9 | 0 | 0 | |
| 10 | 0 | 0 | |
| 11 | 0 | 0 | |
| 12 | 0 | 0 | |
| 13 | 0 | 0 | |

### 3.3.2. Simulation and optimization results

The simulation results corresponding to the matrix presented in Table 4 are summarized in Table 5. The center-point simulations were performed three times with slight variations in the friction coefficient (from 0.08 to 0.12), and the corresponding results are reported in Table 6.

Table 5. Simulation results

| *№* | *1* | *2* | *3* | *4* | *5* | *6* | *7* | *8* |
|---|---|---|---|---|---|---|---|---|
| Y | 40.3 | 41.3 | 21.8 | 25.6 | 27.5 | 33.0 | 43.3 | 22.2 |

Table 6. Results of the center-point simulations

| *№* | *9* | *10* | *11* | *12* | *13* |
|---|---|---|---|---|---|
| Y | 30.0 | 29.8 | 30.1 | 29.9 | 29.7 |

The second-order orthogonal design method was used to evaluate the effects of forming pressure (P) and axial punch velocity (v), as well as the interaction between these factors. The resulting regression equation (4) is:

$$Y=29.9 + 1.572X_1 – 8.006X_2 +0.363X_1^2+1.613X_2^2+0.7\ X_1X_2 \quad (4)$$

According to the statistical analysis, the coefficients of determination $R^2$ and adjusted $R^2_{adj}$ reach 99.16% and 98.55%, respectively, indicating an excellent agreement between the regression model and the simulation data. The included independent variables make statistically significant contributions, and no evidence of overfitting is observed. These results confirm that the proposed regression equation is capable of explaining nearly all of the variability in the dependent variable.

Table 7. Analysis of Variance

| **Source** | **DF** | **Adj SS** | **Adj MS** | **F- Value** | **P-Value** |
|---|---|---|---|---|---|
| Model | 5 | 552.633 | 110.527 | 164.49 | 0.000 |
| Linear | 2 | 532.420 | 266.210 | 396.18 | 0.000 |

| | | | | | |
|---|---|---|---|---|---|
| Forming pressure, p | 1 | 19.776 | 19.776 | 29.43 | 0.001 |
| Punch velocity, v | 1 | 512.644 | 512.644 | 762.92 | 0.000 |
| Square | 2 | 18.254 | 9.127 | 13.58 | 0.04 |
| p*p | 1 | 0.914 | 0.914 | 1.36 | 0.282 |
| v*v | 1 | 18.089 | 18.089 | 26.92 | 0.001 |
| 2-Way interactions | 1 | 1.960 | 1.960 | 2.92 | 0.131 |
| p*v | 1 | 1.960 | 1.960 | 2.92 | 0.131 |
| Lack of Fit | 3 | 4.604 | 1.535 | 61.38 | 0.001 |
| Error | 7 | 4.704 | 0.672 | | |
| Total | 12 | 557.337 | | | |

Table 7 presents the ANOVA results for the obtained regression model. The values P = 0.000 and F = 164.49 indicate that the model is statistically significant and has good predictive capability. Both investigated factors exert certain influences on the product's wall thickness variation. Among them, forming pressure (p) has the smallest impact, while the axial punch speed (v) has the most significant impact. The two-way interaction between forming pressure and punch speed also somewhat affects the wall thickness variation. However, a P-value of 0.131 (> 0.05) reveals that this interaction is not statistically significant. Although the Lack-of-Fit value is statistically significant (P = 0.001), this is common in complex plastic deformation problems due to the high nonlinearity of the material and contact boundary conditions. Nevertheless, the small difference between $R^2$ and $R^2$(adj) (only about 0.61%) confirms that the model is not overfitted and possesses good predictive ability for subsequent optimization studies.

Based on the regression results, the axial punch velocity (v) is identified as the most influential factor on the degree of wall thinning:

**Axial punch velocity ($X_2$)**: A negative regression coefficient (-8.006) indicates that as the punch velocity increases, the degree of wall thinning of the blank significantly decreases. This can be explained by the fact that a high punch velocity helps feed the material into the deformation zone more rapidly, while simultaneously generating axial compressive stress, thereby restricting strain localization that causes localized thinning. The response surface plot (Figure 6) displays a very steep slope along the punch velocity axis, emphasizing that controlling this parameter is crucial to avoid tube wall fracturing defects.

**Forming pressure ($X_1$)**: Contrary to the punch speed, the forming pressure tends to increase the degree of wall thinning (coefficient +1.572). In hydroforming, forming pressure helps the blank fill the die cavity but simultaneously generates large tensile stresses. If the pressure is increased too high without a corresponding material feeding speed from the punch, the tube wall will be excessively stretched, leading to thinning and fracture.

**c) Optimization of wall thickness variation**

From the contour graph in Figure 7, it can be seen that the wall thickness variation gradually increases with increasing axial punch velocity and decreasing forming pressure.

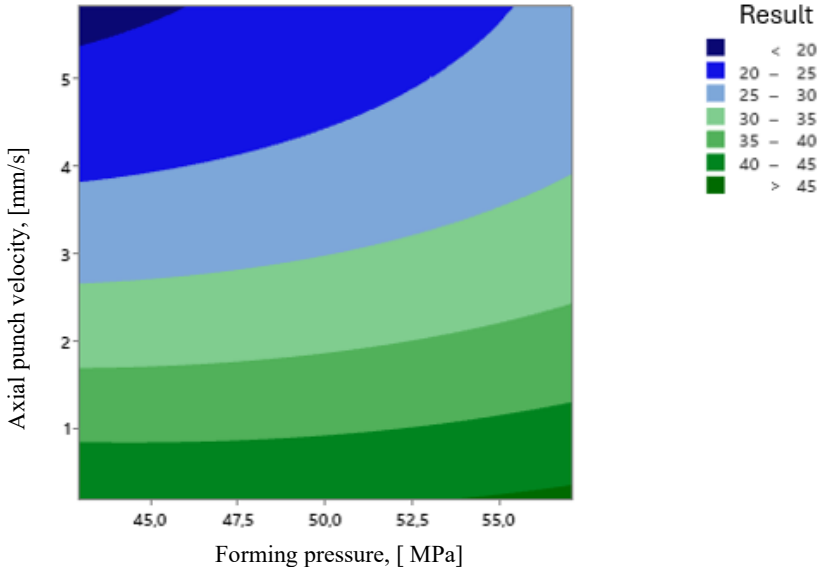


Fig.7. Contour plot of the effect of process parameters on the wall thickness variation

### 3.3.3. Optimization of wall thickness variation

From the contour graph in Figure 7, it can be seen that the wall thickness variation gradually with increasing axial punch velocity and decreasing forming pressure.

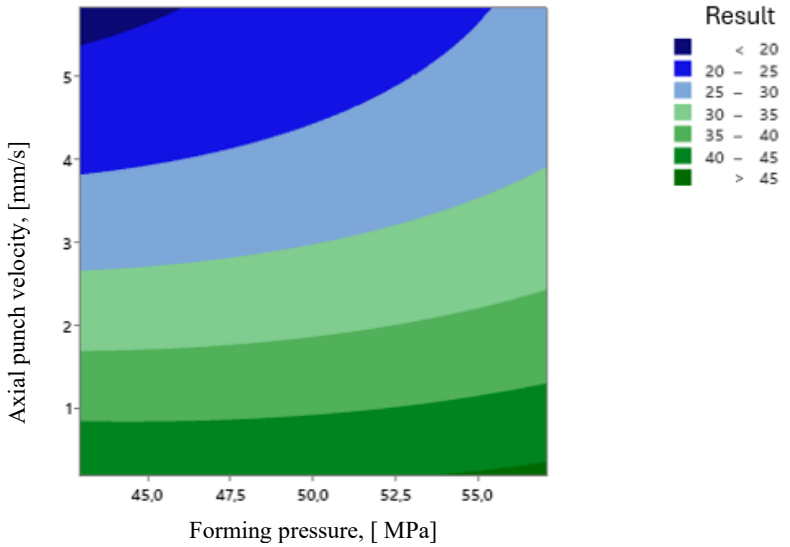


Fig.7. Contour plot of the effect of process parameters on the wall thickness variation

Aiming to obtain a product with a uniform wall thickness (where the wall thickness variation at the spherical section is minimized), the optimal results derived from the analysis show that at a forming pressure of p = 42.9 MPa and a axial punch velocity of v = 5.83 mm/s, the calculated degree of thinning is 18.9%. However, verification through simulations revealed that when the axial punch velocity is excessively high while the forming pressure is low, incomplete die filling occurs. Therefore, to achieve the minimum wall thinning while satisfying the condition of complete die filling without any fracture defects during forming, the appropriate set of process parameters is: forming pressure p = 45 MPa and axial punch velocity v = 5 mm/s. Under these conditions, the degree of wall thinning obtained from the regression equation is 22.1%. This value deviates by 1.4% from the simulation results, demonstrating the high conformity of the model.

## 4. CONCLUSIONS

This study investigates the influence of several technological parameters, such as forming pressure and axial punch velocity, on the die-filling capability and wall thickness variation of necked-spherical parts with collars during the tube hydroforming process using numerical simulation. The results indicate that:

- Forming pressure significantly influences the die-filling capacity. For axial punch velocities ranging from 1 to 5mm/s, the required pressure to ensure complete cavity filling is between 45 and 55 MPa.
- The axial punch velocity plays a dominant role in controlling wall thinning. Increasing the punch velocity from 1 to 5 mm/s results in a substantial reduction in the wall thinning ratio, from 40% to 22.8%.
- The optimal parameters to achieve full cavity filling while minimizing wall thinning are identified as p = 45 MPa and v = 5 mm/s, with this set of values, the wall thickness variation achieved is 22.1%.

Based on the research results, the established processing parameters, including forming pressure and axial punch speed, provide a reliable basis for optimizing product quality, particularly in terms of die filling capability and wall thickness variation, for components with similar geometries. Furthermore, the study identified a critical technological threshold: when the required wall thinning ratio is lower than 22.1%, structural or process modifications should be considered.

**Contributions of Authors:** Nguyen Xuan Diep: Conceptualization, Methodology, Investigation, Visualization, Formal analysis, Writing - original draft, Writing - review & editing. Manh Tien Nguyen: Conceptualization, Methodology, Investigation, Visualization, Formal analysis, Writing - original draft, Writing - review & editing. Truong An Nguyen, Nguyen Xuan Hung, Chu Van Huy: Conceptualization, Methodology, Investigation, Visualization, Formal analysis

**Funding source:** This research was supported by Project No. 25.01.17 from Le Quy Don Technical University.

## 5. REFERENCES


[1]. N.V. Zemlyakova, S.O. Rogachev, (2021), *Shape and dimensions of fragmented bands after cold drawing and intense plastic deformation of the copper*, Probl. Strength Plast., 83(2), 220-226.

[2]. Shijia Wan, Tianhao Yu, Ting Su, Tianchen Yu, Yabin Yan, Fu-Zhen Xuan, (2025), *Effect of high angle grain boundary on plastic deformation and fracture of micro-bicrystal copper: An in-situ SEM experimental and multiscale simulation study*, Mater. Sci. and Eng. A, 942, p.148699.

[3]. S. Atefi, Mohammad Habibi Parsa, Donya Ahmadkhaniha, Caterina Zanella, H.R. Jafarian, (2022*), A study on microstructure development and mechanical properties of pure copper subjected to severe plastic deformation by the ECAP-Conform process*, J. Mater. Res. Technol., 21, 1614-1629.

[4]. N.A. Popova, E.L., Nikonenko, Yu.V., Soloveva, Vladimir Starenchenko, (2024), *Influence of severe plastic deformation on the grain structure and phase composition of technically pure UFG-copper*, Izvestiya vysshikh uchebnykh zavedenii Fizika, 67(12), 201-208.

[5]. Stefan Lechner, Rene Nitschke, Soeren Mueller, (2021), *Numerical analysis of plastic die deformation during high temperature copper extrusion*. ESAFORM 2021. MS03 (Extrusion & Drawing), DOI: 10.25518/esaform21.4785

[6]. Colin Bell, Jonathan Corney, Nicola Zuelli, and David Savings, (2020*), A state of the art review of hydroforming technology: Its applications, research areas, history, and future in manufacturing*, Int. J. Mater. Form., 13(5), 789–828.

[7]. S. Yuan, (2021), *Fundamentals and processes of fluid pressure forming Technology for Complex Thin-Walled Components*, Engineering, 7(3), 358-366, https://doi.org/10.1016/j.eng.2020.08.014.

[8]. M. Koç, T. Altan, (2001), *An overall review of the tube hydroforming (THF) technology*, J. Mater. Pro.Technol., 108(3), 384–393.

[9]. M. Anderson, J., Gholipour, P. Bocher, F. Bridier, J. Savoie & P. Wanjara, (2010), *Formability extension of aerospace alloys for tube hydroforming applications,* Int. J. Mater. Form., 3(S1), 303-306.

[10]. M. Tolazzi, (2010*), Hydroforming applications in automotive: A review*, Int. J. Mater. Form., 3(1), 307–310.

[11]. P. V., Reddy, B.V. Reddy & P.J. Ramulu, (2020), *Evolution of Hydroforming Technologies and its Applications - A Review,* J. Adv. Manuf. Syst., 19(4), 737-780.

[12]. Muammer Koç, (2008), *Hydroforming for advanced manufacturing. 1st edn*, Cambridge England: Woodhead.

[13]. Y.M. Hwang, T.C. Lin, W.C. Chang, (2007), *Experiments on T-shape hydroforming with counter punch*, J. Mater. Process. Technol., 192, 243-248, DOI: 10.1016/j.jmatprotec.2007.04.087.

[14]. Ceclan V., Grozav S., (2018*), Determination of the force required for the hydro forming of al 99,5*, In 3rd International Scientific Conference on Innovative Technologies in Engineering Production (ITEP), 244, pp. 01003.

[15]. X.L. Cui, B. Teng & S. Yuan, (2021), *Hydroforming process of complex T-shaped tubular parts of nickel-based superalloy*, CIRP Journal of Manufacturing Science and Technology, 32, 476-490.

[16]. X. Xu, K. Wu, Y. Wu, X. Jie & C. Fu, (2019), *A novel lubrication method for hydroforming of thin-walled aluminum alloy T-shaped tube*, Int. J. Adv. Manuf. Technol., 102, 2265–2273.

[17]. Vu Duc Quang, Nguyen Dac Trung, Chu Van Huy, Nguyen Huu Toan, Nguyen Anh Tuan, Nguyen Quang Hung, (2022), *Study on the effect of internal pressure and axial feed in tube hydrostatic forming process of T-shaped joints,* Proceedings of the 3rd Annual International Conference on Material, Machines and Methods for Sustainable Development (MMMS2022), Lecture Notes in Mechanical Engineering, pp. 379–391.

[18]. Hongyang Li, Song Yu, Jianhui Li, (2021), *Stress & strain character of tube hydroforming and its application in processing analysis*, IOP Conf. Ser.: Earth Environ. Sci., 714, P. 032090.

[19]. Xuefeng Xu, Yuehui Chen, Xiaoqiang Lei, (2026), *Influence of lubrication method and counter punch on hydroforming in curved diagonal tee tube,* Int. J. Mater. Form., 19, article number 21, https://doi.org/10.1007/s12289-025-01965-w.

[20]. C. Nikhare, Matthias Weiss, Peter Damian, (2017), *Buckling in low pressure tube hydroforming,* J. Manuf. Process., 28, 1-10.

[21]. Chetan P. Nikhare, (2020), *Effect of Thickness on Tube Deformation Mechanics During Low Pressure Tube Hydroforming Process Sequence Variation*, Conference: ASME 2020 International Mechanical Engineering Congress and Exposition, Paper No: IMECE2020-23154, V02AT02A019; 10 pages, https://doi.org/10.1115/IMECE2020-23154

[22]. Yong xu, Xuewei Zhang, Wenlong Xie, Shihong Zhang, Xinyue Huang, Yaqiang Tian, Liansheng Chen, (2024), *Fuzzy Control Optimization of Loading Paths for Hydroforming of Variable Diameter Tubes,* Computers, Materials & Continua. 81, 2753-2768.
[23]. M. T. Trinh, N. D. Trung, P. Q. Tuan, P. N. Anh and D. V. Duy, (2025), *Hydro-Forming a Cross-Shaped Component from Tube Billet,* J. Mach. Eng., 25, 111-122.
[24]. M. T. Trinh, N. D. Trung, P. Q. Tuan, P. N. Anh and D. V. Duy, (2025), *Hydro-forming of U-shaped parts with branches: Stress state and wall thickness analysis*, Engineering, Technology & Applied Science Research, 15(2), 19226-19231.
[25]. Fethi Abbassi, Furqan Ahmad, Sana Gulzar, Touhami Belhadj, Ali Karrech & Heung Soap Choi, (2020*), Design of T-shaped tube hydroforming using finite element and artificial neural network modeling*, J. Mech. Sci. Technol., 34, 1129-1138.
[26]. Zai Xiang Zheng, Jing Xu, Hui Shen, (2012), *Multi-Objective Optimization of the Loading Path in Tube Hydroforming Process Using NCGA*, Appl. Mech. Mater., 217-219, 1885-1889.
[27]. V.D. Quang, (2024), *Study on hydrostatic stamping technology for forming stepped cylindrical and T-shaped hollow parts from tubular blanks*. Dissertation candidate of technical sciences, Ha Noi.
[28]. Chunmei Liu, Ali Abd El-Aty, Myoung-Gyu Lee, Yong Hou, Yong Xu, Shenghan Hu, Cheng Cheng, Jie Tao, Xunzhong Guo, (2023), *Predicting the forming limits in the tube hydroforming process by coupling the cyclic plasticity model with ductile fracture criteria*, J. Mater. Res. Technol., 26, 109-120.
[29]. QuantorForm Ltd. *QForm Material Database: Flow Stress Curves for M1 Copper Alloy*. Version 10.2.4, QuantorForm LLC.
[30]. M.S.J. Hashmi, (2014), *Comprehensive materials processing*, 13, 645-670.

Received: February 09th, 2026 / Accepted: April 18th, 2026 / Paper available online: June 20th, 2026 © International Journal of Modern Manufacturing Technologies.